# Study on end-gas auto-ignition and knock characteristics of ammonia-hydrogen blends over a wide-range equivalence ratios in a rapid compression machine

Qihang Zhang[1], Zhenwei Yang[1], Ridong Zhang[1], Yunliang Qi[1], Zhi Wang[1, *]
[1] School of Vehicle and Mobility, Tsinghua University
Beijing 100084, PR China

## 1 Introduction

Ammonia, a carbon-neutral fuel, has attracted widespread attention for its environmental benefits [1]. However, the low reactivity and combustion inertness of ammonia limit its use as a single fuel in engines. To overcome this limitation, ammonia is commonly blended with highly reactive fuels, such as hydrogen, which is also a zero-carbon fuel [2]. Previous research has demonstrated that even pure ammonia fuels can experience knocking under particular thermodynamic conditions, and the incorporation of hydrogen dramatically elevates the risk of knock [3], which may damage engines severely [4]. Therefore, a comprehensive investigation into the knock characteristics of ammonia-hydrogen blends is essential. In the engines, lean combustion is known to enhance thermal efficiency [4], while hydrogen can be generated from ammonia-rich combustion [5]. This suggests that ammonia-hydrogen fuels are applicable across a broad range of equivalence ratios, but the detailed examination of their knock characteristics across different equivalence ratios is a field that has not yet been fully explored. Under such a background, the current study employs optical visualization techniques to examine the knocking combustion properties of ammonia-hydrogen fuels at varying equivalence ratios and with different proportions of hydrogen.

## 2 Experimental Setup

### 2.1. Rapid compression machine system

The experiments were conducted at Tsinghua University using a rapid compression machine (TU-RCM) with a 50.8 mm diameter combustion chamber and 500 mm stroke. A creviced piston and quartz window (JGS-1) were used for temperature uniformity and visualization, as shown in Figure 1 (a). The combustion process was recorded using a Photron SA-X2 high-speed camera equipped with a 50 mm Nikon lens at a resolution of 128×128, a frame rate of 288,000 fps and a shutter speed ranging from 0.293 to 1.250 μs. The pressure data were measured by a Kistler 6125C pressure transducer and NI cDAQ-9178 system at a sampling frequency of 100 kHz. Further details on the TU-RCM and its control system are available in reference [6].

Correspondence to: wangzhi@tsinghua.edu.cn

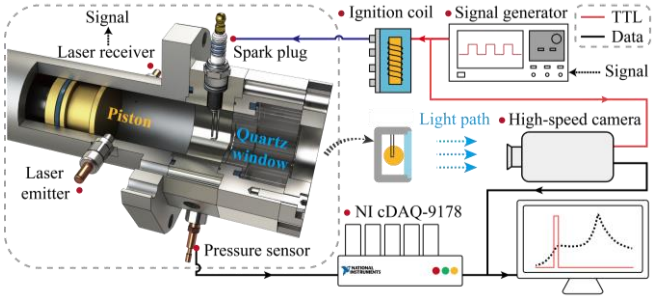


Figure 1: TU-RCM system and a typical pressure trace of the experiments

### 2.2. Mixtures and test conditions

The thermodynamic conditions of the test mixtures are characterized by the pressure ($p_{EOC}$) and temperature ($T_{EOC}$) at the end of compression (EOC). Parameter definitions are available in reference [6]. Table 1 shows the mixture compositions and test conditions. Ammonia, hydrogen, oxygen, nitrogen, and argon mixtures at equivalence ratios of 0.4/ 0.7/ 1/ 1.5/ 2 were used in the experiments. The mixtures were categorized based on the relative molar ratio of ammonia and hydrogen: H0 (pure ammonia), H5 (5% hydrogen, 95% ammonia), and H20 (20% hydrogen, 80% ammonia). $p_{EOC}$ was set to 30 bar and $T_{EOC}$ was set to 900 K.

Table 1: Mixture composition and test conditions

| $n_{H2}/ (n_{H2}+ n_{NH3})$ | $p_{eff}$ (bar) | $T_{eff}$ (K) | Equivalence ratio $\varphi$ | Dilution ratio （Molar ratio of buffer gas to $O_2$） | Ar/ $N_2$ molar ratio |
|---|---|---|---|---|---|
| 0 (H0)/ 5 (H5)/ 20 % (H20) | 30 | 900 | 0.4/ 0.7/ 1/ 1.5/ 2 | 3.76 (Ar+$N_2$) | 1.5 |

## 3 Results and discussions

### 3.1. Knock intensity

In this study, H0 exhibited no knocking across all equivalence ratios. H5 encountered knocking exclusively at equivalence ratios of 1, 1.5, and 2. In contrast, H20 experienced knocking under all tested operating conditions. The parameters $dp_{max}$ and *KI* (Knock Intensity) are employed to quantify the intensity of knock. $dp_{max}$ denotes the peak amplitude of the pressure oscillations, whereas *KI* is the integral value over the high-pass filtered pressure oscillations. Detailed definitions can be found in the reference [7].

As shown in Figure 2, with a fixed fuel ratio, both $dp_{max}$ and *KI* exhibit bell-shaped and achieved the peak values at an equivalence ratio of 1, indicating that knock intensity was most severe at this condition, whereas both lean and rich combustion resulted in a decreased knock intensity. At a constant equivalence ratio, both $dp_{max}$ and *KI* of H20 are larger than H5, suggesting that the knock tendency increases with the higher hydrogen proportion.

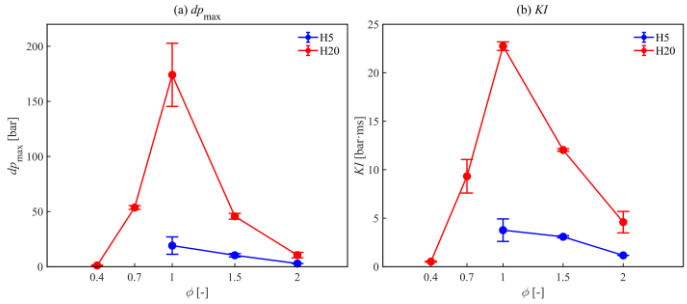


Figure 2: The results of $dp_{max}$ and $KI$

### 3.2. Factors affecting knock

Previous studies [7] have demonstrated that knock intensity exhibits a robust correlation with several parameters: the residence time, defined as the duration from ignition to the onset of auto-ignition, the burned mass fraction (*BMF*), a metric used to quantify the proportion of the end-gas, and the energy density ($E_{eg}$), a parameter used to characterize the thermodynamic state of end-gas. Detailed definitions can be found in the reference [8]. For H5, knock did not occur at equivalence ratios below 1, so there were no *BMF*, recorded residence times, or $E_{eg}$ in these conditions.

As illustrated in Figure 3, with a fixed fuel ratio, the residence time presents a U-shaped pattern and reaches its lowest value at an equivalence ratio of 1, with both lean and rich combustion leading to an increase in residence time. In contrast, both the *BMF* and $E_{eg}$ exhibit bell-shaped and achieves the highest values at an equivalence ratio of 1, and deviations towards either leaner or richer conditions result in a decrease of the *BMF* and $E_{eg}$. At a constant equivalence ratio, the residence time, the *BMF*, and the $E_{eg}$ exhibit an upward trend with the decreasing proportion of hydrogen.

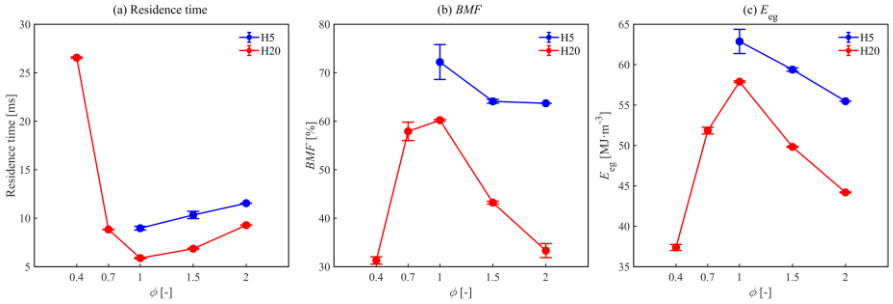


Figure 3: The results of *BMF*, residence time, and $E_{eg}$

Figure 4 illustrates the interplay between $dp_{max}$ and the parameters of residence time, *BMF*, and $E_{eg}$. At a constant fuel ratio, a negative correlation is observed between residence time and knock intensity. Conversely, a positive correlation is evident among *BMF*, $E_{eg}$ and knock intensity. This can be attributed to the enhanced reactivity of the mixture as it approaches the equivalence ratio of 1, which accelerates flame velocities and ensures a more thorough combustion process. As a result, the residence times are reduced, while the *BMF* and $E_{eg}$ are increased. However, the enhanced reactivity also increases the knock intensity.

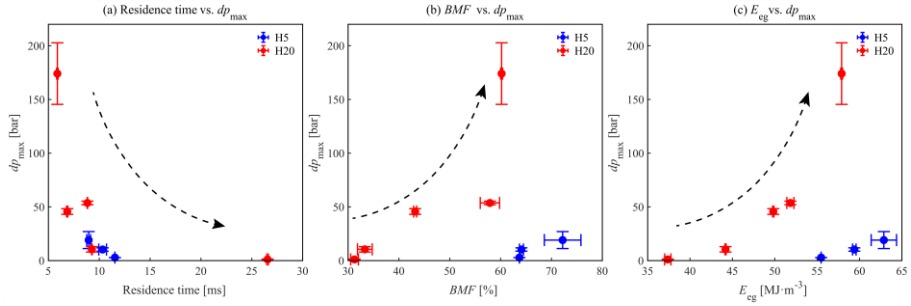


Figure 4: Knock intensity against three parameters

### 3.3. Visualization results

Figure 5 presents the visualization results of flame and auto-ignition for H0, H5, and H20 across various equivalence ratios. The brightness enhancement factor, indicated in the lower right corner of each image, facilitates a clearer visualization of the auto-ignition process, while the time below each image is the time after spark ignition. The flame colors observed for H0, H5, and H20 at different equivalence ratios exhibit notable variations, a finding that reported in our earlier research [6]. The insights from spectral analysis were provided to elucidate this phenomenon. It is evident that auto-ignition (A.I.) in the H5 mixture is confined to equivalence ratios of 1, 1.5, and 2, whereas the H20 mixture experiences auto-ignition at all the equivalence ratios. Notably, all the auto-ignition regions exhibit a more vibrant yellow compared to flame at the auto-ignition moment, which may be attributed to the luminescence of $NH_2$ radicals [9]. For H20 at an equivalence ratio of 1, auto-ignition was followed by the onset of detonation merely 0.004 ms later, at 6.028 ms after spark ignition. A distinct detonation wave (Deto.) is observed, as depicted in Figure 5 (c3).

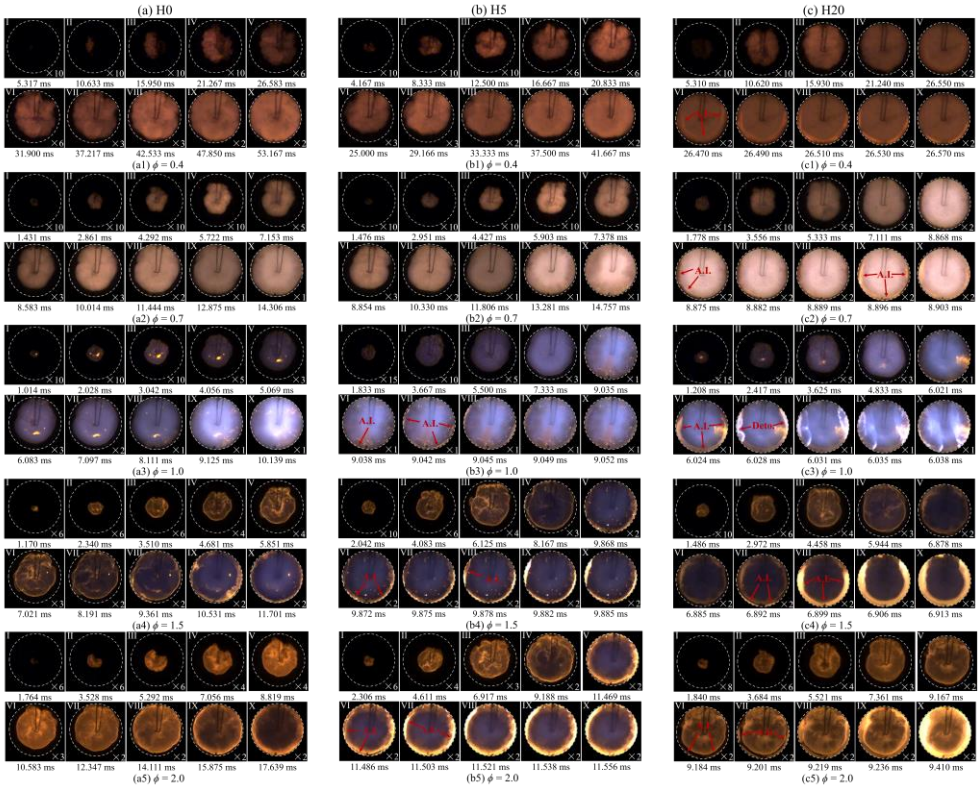


Figure 5: The images of flame and auto-ignition at $T_{EOC}$=900 K

The images are processed to show auto-ignition within the end-gas region clearly, as illustrated in Figure 6. For each mixture at different equivalence ratios, the top row of images represents the original high-speed captures, while the bottom row displays the corresponding images after background subtraction. At the same equivalence ratio, the end-gas region is more extensive in H20 compared to H5, consistent with the *BMF* results. This is because the competition between the consumption of end-gas by the flame and the compression heating of the end-gas [3]. For H20, the flame has elevated the end-gas to thermodynamic conditions sufficient for auto-ignition to occur before it has consumed the end-gas to a small amount. The enlarged end-gas region promotes auto-ignition across a broader area, leading to the observation of contiguous (Conti.) auto-ignition patches in the H20 images. This enhanced the knock intensity. In contrast, the end-gas of H5 is consumed to a small volume or even fragmented by the time auto-ignition occurs, resulting in a multi-regional (Multi.), small-scale auto-ignition event, which consequently leads to a lower knock intensity. The similar result has been observed in the previous study of iso-octane [7]. However, for H20 at an equivalence ratio of 0.4, auto-ignition did not manifest in patches due to the high dilution of the mixture.

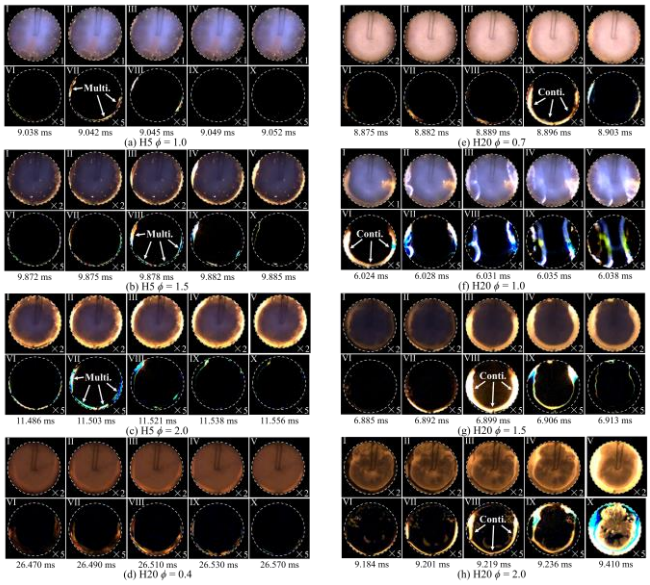


Figure 6: The auto-ignition process

More conclusions will be drawn in future studies, including thermodynamic analysis and chemical analysis.

## 4 Conclusions

This work investigates the spark-ignition combustion process and the end-gas auto-ignition behavior of ammonia-hydrogen blends using an optical RCM. The equivalence ratios of the test mixtures were set to 0.4/ 0.7/ 1/ 1.5/ 2 and the experiments were conducted at the conditions of $p_{EOC}$ = 30 bar, $T_{EOC}$ = 900 K. The main conclusions are as follows:

(1) With a constant fuel ratio, both $dp_{max}$ and *KI* exhibit bell-shaped curves, peaking at an equivalence ratio of 1, suggesting that the most severe knock occurred at this ratio, with lean and rich mixtures showing reduced knock intensity. The knock intensity increases as hydrogen proportion increases.

(2) The residence time presents a U-shaped pattern, while *BMF* and $E_{eg}$ exhibit bell-shaped, with the extreme values occurring at an equivalence ratio of 1. All the three parameters decrease as hydrogen proportion increases. *BMF* and $E_{eg}$ positively correlate with knock intensity, whereas residence time correlates negatively.

(3) Due to the competition between end-gas consumption and compression heating by the flame, the end-gas region of H20 is larger than H5, leading to broader auto-ignition and higher knock intensity, while the end-gas of H5 is largely consumed before auto-ignition, resulting in multi-regional auto-ignition and reduced knock intensity.

## Acknowledgements

This study was supported by the National Natural Science Foundation of China (Grant Nos.: T2241003, T2341002, and 52076118).

## References

[1] G. Kalghatgi, H. Levinsky, M. Colket, Future transportation fuels, Progress in Energy and Combustion Science 69 (2018) 103-105.
[2] Z. Wang, Y. Qi, Q. Sun, Z. Lin, X. Xu, Ammonia combustion using hydrogen jet ignition (AHJI) in internal combustion engines, Energy 291 (2024).
[3] R. Zhang, Q. Zhang, Y. Qi, B. Yang, Z. Wang, Investigation on flame propagation and end-gas auto-ignition of ammonia/hydrogen in a full-field-visualized rapid compression machine, Proc. Combust. Inst. 40 (2024).
[4] Z. Wang, H. Liu, R.D. Reitz, Knocking combustion in spark-ignition engines, Progress in Energy and Combustion Science 61 (2017) 78-112.
[5] W. Liu, Y. Qi, R. Zhang, Q. Zhang, Z. Wang, Hydrogen production from ammonia-rich combustion for fuel reforming under high temperature and high pressure conditions, Fuel 327 (2022).
[6] Q. Zhang, Y. Qi, R. Zhang, X. Chao, B. Yang, Z. Wang, Chemiluminescence spectra investigation of ammonia flame over a wide-range equivalence ratios in a rapid compression machine, Fuel 382 (2025).
[7] W. Liu, Y. Qi, X. He, Z. Wang, Investigation on Effects of Ignition Configurations on Knocking Combustion Using an Optical Rapid Compression Machine under Lean to Stoichiometric Conditions, Combustion Science and Technology 194 (2020) 1678-1699.
[8] R. Zhang, W. Liu, Q. Zhang, Y. Qi, Z. Wang, Auto-ignition and knocking combustion characteristics of iso-octane-ammonia fuel blends in a rapid compression machine, Fuel 352 (2023).
[9] A. Hayakawa, T. Goto, R. Mimoto, Y. Arakawa, T. Kudo, H. Kobayashi, Laminar burning velocity and Markstein length of ammonia/air premixed flames at various pressures, Fuel 159 (2015) 98-106.